Three-dimensional ordering in weakly coupled antiferromagnetic ladders and chains

Stefan Wessel and Stephan Haas
Department of Physics and Astronomy, University of Southern California, Los Angeles, California 90089-0484
(Received 15 February 2000)

A theoretical description is presented for low-temperature magnetic-field-induced three-dimensional (3D) ordering transitions in strongly anisotropic quantum antiferromagnets, consisting of weakly coupled antiferromagnetic spin-1/2 chains and ladders. First, effective continuum field theories are derived for the one-dimensional subsystems. Then the Luttinger parameters, which determine the low-temperature susceptibilities of the chains and ladders, are calculated from the Bethe ansatz solution for these effective models. The 3D ordering transition line is obtained using a random-phase approximation for the weak interchain (interladder) coupling. Finally, considering a Ginzburg criterion, the fluctuation corrections to this approach are shown to be small. The nature of the 3D ordered phase resembles a Bose condensate of integer-spin magnons. It is proposed that for systems with higher spin degrees of freedom, e.g., *N*-leg spin-1/2 ladders, multicomponent condensates can occur at high magnetic fields.

I. INTRODUCTION

Compounds of weakly coupled spin chains typically have an ordering transition from a high-temperature quasi-one-dimensional (1D) phase to a low-temperature three-dimensional (3D) phase at a critical temperature that depends on the interchain coupling constant.[1] This transition can be suppressed if the individual chains are gapped spin liquids, as it is the case for Haldane or spin-Peierls systems, or for compounds with an Ising anisotropy in the intrachain exchange coupling. In these systems, the low-energy spectrum consists of a singlet ground state with an excitation gap to the first triplet. This gap can be reduced and eventually overcome by turning on and increasing an external magnetic field. Once the spin gap is destroyed, the residual interchain coupling can lead to 3D ordering at low temperatures.[2–4] In this paper, we discuss a quantitative theoretical approach to study such magnetic-field-induced transitions, based on an exact field-theoretical description of the low-energy intrachain dynamics that drives the transition, combined with a mean-field theory (including quantum fluctuation corrections) for the interchain exchange.

Our results are in good agreement with recent experiments on the compounds $TlCuCl_3$ (Ref. 5) and $Cu_2(C_2H_{12}N_2)_2Cl_4$,[6] where transition lines $h_c(T)$ were extracted from an analysis of the temperature-dependent magnetization and from NMR data for the $1/T_1$ relaxation. Typically, the spin gap in most of the ladder compounds known to date is too large to be overcome by presently available magnetic fields. However, these particular materials have small spin gaps of the order 10–20 K, which makes the interesting gapless regime experimentally accessible. It has recently been pointed out that $Cu_2(C_2H_{12}N_2)_2Cl_4$ may better be modeled as an ensemble of weakly coupled dimers than as an antiferromagnetic two-leg ladder.[7] Whatever the precise structure may turn out to be, a magnetic-field-induced ordering transition can occur in all anisotropic spin systems with a singlet-triplet excitation gap, including weakly coupled Ising-like chains, spin-Peierls chains, and ensembles of spin dimers. Other possible candidate materials with spin gaps include $KCuCl_3$,[8] $CuGeO_3$,[9] α'-NaV_2O_5,[10] and the homologous series of cuprates $Sr_nCu_{n+1}O_{2n+1}$.[11]

The exact nature of these 3D ordered phases is currently under debate.[4,5] In the case of weakly coupled gapless chains that undergo a 3D ordering transition even in the absence of a magnetic field, long-range antiferromagnetic order is found below the transition temperature.[1] For the spin-gapped compounds $TlCuCl_3$ and $Cu_2(C_2H_{12}N_2)_2Cl_4$ the field-induced low-temperature transition resembles that of a Bose-Einstein condensation of integer-spin magnons. The critical exponent for the transition line of such a condensate, i.e., $h_c \propto T^\alpha$ with $\alpha = 3/2$, is rather close to the experimentally observed behavior.[4,5]

In this work, a numerical solution of the Bethe ansatz is used to determine the susceptibilities of the one-dimensional subsystems, combined with a generalized random-phase approximation (RPA) approach for the low-temperature 3D ordering transition. In the following section, we illustrate this approach by discussing the case of weakly coupled Heisenberg chains with an easy-axis anisotropy (*XXZ* model). Subsequently, corrections due to fluctuation effects are determined, which turn out to be rather small. Then the case of weakly coupled two-leg ladders and dimerized chains in a magnetic field is discussed. These results are most pertinent to recent and forthcoming experiments. Finally, we examine weakly coupled *N*-leg ladders with $N > 2$. In this case, multiple ordering transitions can occur, which may partially overlap. In our conclusions, we propose that these overlapping high-field phases are multicomponent Bose-Einstein condensates, consisting of magnons with different integer spin.

II. SPIN-1/2 HEISENBERG CHAINS

Let us consider a crystal of weakly coupled antiferromagnetic Heisenberg chains in a magnetic field, described by the Hamiltonian

$$H^{1D} = \sum_i \left[J(S_i^x S_{i+1}^x + S_i^y S_{i+1}^y + \Delta S_i^z S_{i+1}^z) - h S_i^z \right], \quad (1)$$

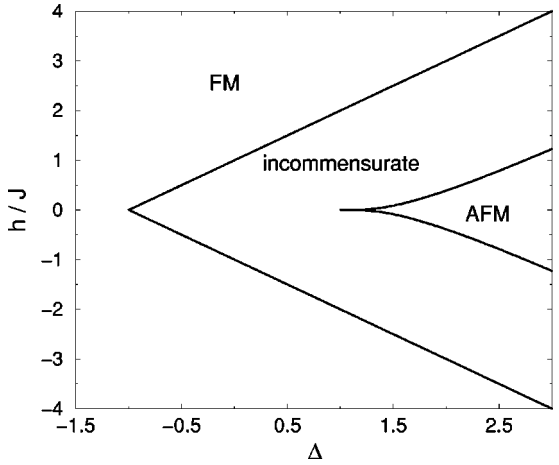

FIG. 1. Phase diagram of a spin-1/2 Heisenberg chain with an easy-axis anisotropy Δ, in a magnetic field h. FM, ferromagnetic regime; incommensurate, partially polarized gapless regime; AFM, antiferromagnetic regime.

where $J>0$ is an antiferromagnetic exchange constant within the chains, Δ is an easy-axis anisotropy, and h is an applied external magnetic field. The chains are weakly coupled by $H'=J'\Sigma_{\langle i,j\rangle}\mathbf{S}_i\cdot\mathbf{S}_j$ with $0<J'\ll J$.

The phase diagram of H^{1D} can be obtained from a numerical solution of the Bethe ansatz equations,[12,13] and is shown in Fig. 1. At zero magnetic field, the 1D subsystem is in the ferromagnetic Ising regime for $\Delta<-1$. In the interval $-1<\Delta<1$, it is in the gapless XY regime, whereas for $\Delta>1$, it is in the massive Ising antiferromagnetic regime. The magnetization of the system becomes nonzero if the magnetic field h exceeds a minimal field given by $h_{min}=0$ for $-1<\Delta<1$. In the gapped case ($\Delta=\cosh\gamma\geqslant 1$):

$$h_{min}=J\frac{2\pi\sinh\gamma}{\gamma}\sum_{n=0}^{\infty}\frac{1}{\cosh\dfrac{(2n+1)\pi^2}{2\gamma}}. \tag{2}$$

It saturates at a maximum critical field given by $h_{\max}=(1+\Delta)J$.

The interchain coupling J' is assumed to be small compared to the intrachain coupling J. Therefore, 3D long-range antiferromagnetic order only occurs in the gapless region. In order to calculate the magnetic response of the chains and the 3D ordering temperature, one needs to know the low-temperature behavior of the susceptibility at finite magnetic fields. This can be determined analytically by mapping H^{1D} onto an effective continuum field theory that describes the low-lying excitations of H^{1D} in the gapless incommensurate regime. For Δ close to zero, the long-wavelength limit of H^{1D} can be studied via bosonization techniques, leading to a $c=1$ conformal field theory (CFT). The effective parameters of this CFT for the *whole range* of Δ can be determined by comparing the thermodynamical properties of this CFT with the numerical Bethe ansatz solution to the original Hamiltonian (1).

In the following, we discuss the technical aspects of this procedure. The Hamiltonian (1) can be mapped onto a model of interacting spinless fermions via a Wigner-Jordan transformation[14]

$$S_i^+=S_i^x+iS_i^y=a_i^\dagger\exp\left(i\pi\sum_{j=1}^{i-1}a_j^\dagger a_j\right),\quad S_i^z=a_i^\dagger a_i-\frac{1}{2}. \tag{3}$$

Using the fact that $H^{1D}(J,\Delta,h)$ is related to $H^{1D}(-J,-\Delta,h)$ via a unitarity transformation, this mapping gives

$$\begin{aligned}H_F^{1D}=&-J\sum_{k\in\mathrm{BZ}}a_k^\dagger a_k\cos k+\left(\Delta+\frac{h}{J}\right)a_k^\dagger a_k\\&+\frac{\Delta J}{N}\sum_{k_1,\ldots,k_4}\delta(k_1+k_3-k_2-k_4)\\&\times e^{i(k_1-k_4)}a_{k_1}^\dagger a_{k_2}a_{k_3}^\dagger a_{k_4}.\end{aligned} \tag{4}$$

The magnetization of the chain, m, is related to the spinless fermion density n by $m=n-1/2$. Hence, the lower critical field h_{c1}^e is determined by the condition that the band of spinless fermions starts to fill up. Since in this low-density limit the interactions between the fermions are negligible, one easily finds $h_{c1}^e=-(1+\Delta)J_e$. From a particle-hole transformation $a_k^\dagger\rightarrow b_k$, the upper critical field $h_{c2}^e=(1+\Delta)J_e$ (high-density limit for the spinless fermions) is obtained analogously.

In the gapless region (i.e., $h_{c1}\leqslant h\leqslant h_{c2}$), we bosonize H^{1D} and obtain a $c=1$ CFT of a compactified scalar field,

$$H_B=\int dx\left(\frac{\pi uK}{2}\Pi^2+\frac{u}{2\pi K}(\partial_x\phi)^2\right), \tag{5}$$

where $\phi(x,t)$ is the bosonic field and $\Pi(x,t)$ is its conjugate momentum. The Luttinger parameters K and u depend on the magnetic field and the exchange interaction of the original Hamiltonian, and still need to be determined. One can interpret H_B as describing a compactified boson with radius

$$R=\frac{1}{\sqrt{4\pi K}}. \tag{6}$$

We will now discuss the equations to determine K and u, which can be derived from the Bethe ansatz for H^{1D} (see, e.g., Ref. 15). One finds a system of integral equations[13,16] that need to be solved numerically. The dressed energy $\epsilon_d(\eta)$ satisfies the integral equation

$$\epsilon_d(\eta)=\epsilon_0(\eta)-\frac{1}{2\pi}\int_{-\Lambda}^{\Lambda}K(\eta-\eta')\epsilon_d(\eta')d\eta', \tag{7}$$

where the kernel $K(\eta)$ and the bare energy $\epsilon_0(\eta)$ are given in Table I.[17] A similar table has been given by Cabra *et al.*[13]

The cutoff parameter Λ is determined by the condition

$$\epsilon_d(\Lambda)=0. \tag{8}$$

Once Λ has been obtained, the dressed charge function $\xi(\eta)$ can be calculated from the integral equation

$$\xi(\eta)=1-\frac{1}{2\pi}\int_{-\Lambda}^{\Lambda}K(\eta-\eta')\xi(\eta')d\eta', \tag{9}$$

directly giving the Luttinger exponent K:

TABLE I. Functions used in the integral equations for the XXZ chain.

Δ	$K(\eta)$	$\epsilon_0(\eta)$	$g(\eta)$
$\cos\theta=\Delta<1$	$\dfrac{\tan\theta}{\tan^2\theta\cosh^2\dfrac{\eta}{2}+\sinh^2\dfrac{\eta}{2}}$	$\dfrac{h}{J}+\dfrac{\Delta^2-1}{\cosh\eta-\Delta}$	$\dfrac{\cot\dfrac{\theta}{2}}{\cosh^2\dfrac{\eta}{2}+\cot^2\dfrac{\theta}{2}\sinh^2\dfrac{\eta}{2}}$
$\Delta=1$	$\dfrac{4}{\eta^2+4}$	$\dfrac{h}{J}-\dfrac{2}{\eta^2+1}$	$\dfrac{2}{\eta^2+1}$
$\cosh\gamma=\Delta>1$	$\dfrac{\tanh\gamma}{\tanh^2\gamma\cos^2\dfrac{\eta}{2}+\sin^2\dfrac{\eta}{2}}$	$\dfrac{h}{J}+\dfrac{\Delta^2-1}{\cos\eta-\Delta}$	$\dfrac{\coth\dfrac{\gamma}{2}}{\cos^2\dfrac{\eta}{2}+\coth^2\dfrac{\gamma}{2}\sin^2\dfrac{\eta}{2}}$

$$K=\xi(\Lambda)^2. \tag{10}$$

Simultaneously, the integral equations for the phase-space densities $\sigma(\eta)$ and $\rho(\eta)$ are solved self-consistently:

$$\sigma(\eta)=g(\eta)-\frac{1}{2\pi}\int_{-\Lambda}^{\Lambda}K(\eta-\eta')\sigma(\eta')d\eta', \tag{11}$$

$$\rho(\eta)=\frac{1}{2\pi}\frac{dK(\eta-\Lambda)}{d\eta}-\frac{1}{2\pi}\int_{-\Lambda}^{\Lambda}K(\eta-\eta')\rho(\eta')d\eta'. \tag{12}$$

Then the spinon velocity u and the magnetization m are given by

$$\frac{u}{J}=\frac{e}{2\pi\sigma(\Lambda)}, \tag{13}$$

$$m=1-2\int_{-\Lambda}^{\Lambda}\sigma(\eta)d\eta, \tag{14}$$

where

$$e=\frac{d\epsilon_0(\Lambda)}{d\Lambda}+\int_{-\Lambda}^{\Lambda}\epsilon_0(\eta)\rho(\eta)d\eta. \tag{15}$$

In Fig. 2, the magnetization curves $m(h)$ for an XY-like, an isotropic, and an Ising-like Heisenberg chain are shown, along with the upper and lower bound of the spinon excitation spectrum. The cases $\Delta=0.5$ and $\Delta=1.0$ are gapless, whereas for $\Delta=2.0$, the zero-field spin gap [Fig. 3(f)] leads to a plateau in $m(h)$ [Fig. 3(c)]. Furthermore, the bandwidth of the spinon spectrum increases with Δ, reflecting the renormalization of the spinon velocity due to backscattering processes.

From the exact numerical solution of the continuum model, the spin-spin correlation functions of the original model (1) can be derived. In turn, the finite-temperature susceptibilities are given via a Fourier transformation of the correlation functions.[18] The low-temperature behavior of the susceptibility in the gapless regime is determined by the dominant low-frequency spinon modes at momentum $q_z=\pi$:[4,19]

$$\chi^{1D}_{+-}(q_z,\omega=0;T)=F(\Delta)\left[\frac{\sin\left(\dfrac{\pi}{4K}\right)}{u}\left(\frac{2\pi T}{u}\right)^{1/2K-2}\times B^2\left(\frac{1}{8K},1-\frac{1}{4K}\right)-\frac{\pi}{u(1-1/4K)}\right], \tag{16}$$

where $B(x,y)$ is Euler's beta function, and $F(\Delta)$ is a prefactor that strongly depends on the Ising anisotropy:[20]

$$F(\Delta)=\frac{1}{2(1-\beta^2)^2}\left[\frac{\Gamma\left(\dfrac{\beta^2}{2-2\beta^2}\right)}{\sqrt{\pi}\Gamma\left(\dfrac{1}{2-2\beta^2}\right)}\right]^2 \tag{17}$$

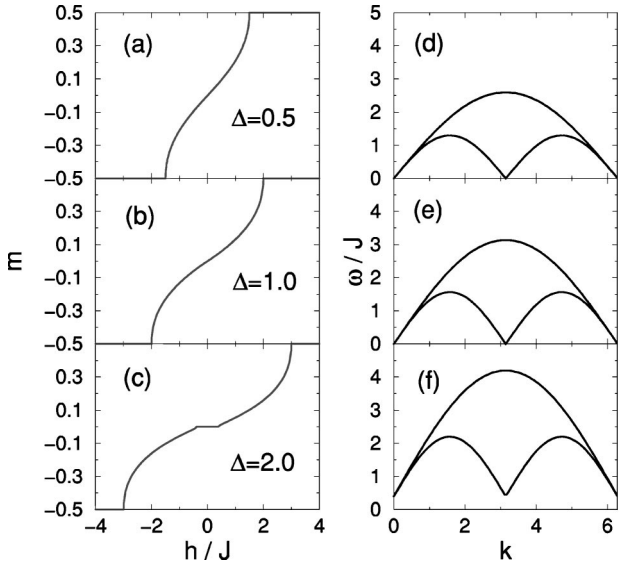

FIG. 2. (a)–(c): Magnetization curves $m(h)$ of an antiferromagnetic spin-1/2 XXZ chain. (a) XY regime with Ising anisotropy $\Delta=0.5$, (b) isotropic Heisenberg point with $\Delta=1.0$, and (c) Ising regime with $\Delta=2.0$. The graphs in (d)–(f) show the corresponding lower and upper bounds of the spinon excitation spectrum, $\omega(k)$.

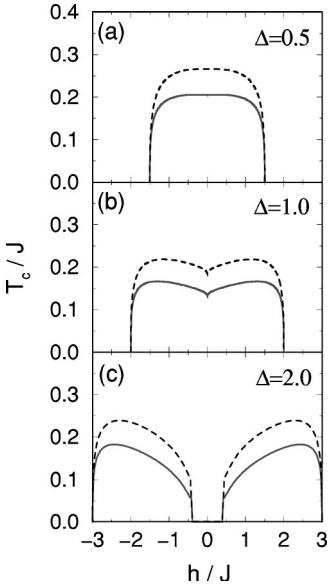

FIG. 3. 3D ordering temperature (solid line) as a function of the applied magnetic field in a cubic crystal of weakly coupled antiferromagnetic spin-1/2 XXZ chains. (a) XY regime with $\Delta=0.5$, (b) Heisenberg point ($\Delta=1.0$), and (c) Ising regime with $\Delta=2.0$. The dashed lines indicate the onset of the fluctuation region below which the 3D magnetic correlation length becomes comparable to the interchain spacing. For this plot, we have chosen $J'/J=1/16$.

$$\times\exp\left\{-\int_0^\infty\frac{dt}{t}\left(\frac{\sinh(\beta^2 t)}{\sinh t\cosh[(1-\beta^2)t]}-\beta^2 e^{-2t}\right)\right\}, \tag{18}$$

where $\cos(\pi\beta^2)=\Delta$. Here, it has been assumed that the chains are parallel to the z axis of the crystal. Furthermore, we have neglected higher-order logarithmic corrections that arise in a more rigorous treatment of the backscattering processes.

The low-temperature transition line to 3D ordering due to the small but finite inter-chain coupling J' can be calculated within an RPA approximation. The corresponding 3D susceptibility is then given by[1,21]

$$\chi^{3D}(\mathbf{q},\omega=0;T)=\frac{\chi^{1D}(q_z,\omega=0;T)}{1+J'f(\mathbf{q})\chi^{1D}(q_z,\omega=0;T)}, \tag{19}$$

where $f(\mathbf{q})$ is the crystal form factor, which we here set to $f(\mathbf{q})=-1$ for simplicity (simple cubic lattice). The 3D ordering transition is driven by the low-temperature divergence of $\chi^{1D}(q_z,\omega=0;T)$, where the transition temperature is given by the locus of the divergence of $\chi^{3D}(\mathbf{q},\omega=0;T)$. The resulting magnetic-field dependence of T_c is shown in Fig. 3 for the various regimes of Δ. The field dependence of the onset of the crossover from 1D to 3D is shown by the dashed line, which is obtained from the fluctuation formula derived in the next section.

In this section, we have calculated the Luttinger parameters (K and u) of the effective CFT (5) for the XXZ chain from a numerical solution of the Bethe ansatz equations within the whole range of Δ. However, the particular case of the XY limit ($\Delta=0$) can be treated *exactly* via bosonization (after linearization of the dispersion law around the Fermi points), since the corresponding fermionic theory is free in this case. In this limit, one finds the following values for u and K:

$$\frac{u}{J}=v_F=\sqrt{1-\left(\frac{h}{J}\right)^2}, \quad K=1. \tag{20}$$

In this limit, the 3D transition temperature is

$$T_c=Jv_F^{1/3}C_1\left[\frac{J}{J'}+C_2\frac{1}{v_F}\right]^{-2/3}, \tag{21}$$

where C_1 and C_2 are given numerical constants. At the lower critical field $h_{c1}=-1$ the behavior of T_c is thus $T_c\propto\sqrt{h-h_{c1}}$.[22] From the numerical results, a similar scaling behavior at the edge of the gapless phase is obtained for nonzero values of Δ.

III. GINZBURG CRITERION

To determine the quality of the RPA theory described in the previous section, a Ginzburg criterion will now be used to examine the width ΔT_c of the critical region. This can be done within the spinless fermion picture of the coupled chains, for which a Landau-Ginzburg functional can be derived. Denoting the localized spins by $\mathbf{S}_{i\mu}$, where the index μ labels the 1D chains and the index i the position along these chains, the Hamiltonian for the entire 3D system is given by

$$H^{3D}=\sum_\mu H_\mu^{1D}(J,\Delta,h)+J'\sum_{i,\langle\mu,\nu\rangle}\mathbf{S}_{i\mu}\cdot\mathbf{S}_{i\nu}. \tag{22}$$

Introducing spinless-fermion creation operators on each chain, this Hamiltonian can be mapped onto a model of weakly coupled metallic chains. Neglecting the interchain hopping (assuming an Ising-like coupling between the chains), the resulting Hamiltonian is

$$\begin{aligned}H_F^{3D}=&-J\sum_{k,\mu}a_{k\mu}^\dagger a_{k\mu}\cos k+\left(\Delta+\frac{h}{J}-\frac{J'}{J}\right)a_{k\mu}^\dagger a_{k\mu}\\&+\frac{J\Delta}{N}\sum_{k_1,\ldots,k_4,\mu}\delta(k_1+k_3-k_2-k_4)\\&\times e^{i(k_1-k_4)}a_{k_1\mu}^\dagger a_{k_2\mu}a_{k_3\mu}^\dagger a_{k_4\mu}-\frac{J'}{N}\sum_{k_1,\ldots,k_4,\langle\mu,\nu\rangle}\\&\times\delta(k_1+k_3-k_2-k_4)a_{k_1\mu}^\dagger a_{k_2\mu}a_{k_3\nu}^\dagger a_{k_4\nu}\end{aligned} \tag{23}$$

Note that the interchain coupling renormalizes the bare chemical potential. After linearization of the dispersion around the Fermi points, one finds a generalized Landau-Ginzburg functional, describing the 3D ordering transition of the original model in terms of a density-wave-type phase transition within the spinless fermion picture:

$$\begin{aligned}F[\Psi(x,y,z)]=\frac{1}{d_\perp^2}\int d^3x[&A|\Psi|^2+B|\Psi|^4+C_\perp|\nabla_\perp\Psi|^2\\&+C_\parallel|\nabla_\parallel\Psi|^2].\end{aligned} \tag{24}$$

Here $d_\perp$ denotes the interchain distance, and the other parameters can be expressed in terms of those of the microscopic model. Analogous to Ref. 23, they are

$$A=\frac{1-J\chi^{1D}(q_z,\omega=0;T)}{\chi^{1D}(q_z,\omega=0;T)}, \tag{25}$$

$$B=\frac{v}{2}\frac{7\zeta(3)}{8\pi}\frac{\gamma^2}{T^2}J^3\chi^{1D}(q_z,\omega=0;T), \tag{26}$$

$$C_\perp=\frac{1}{2}Jd_\perp^2, \tag{27}$$

$$C_\parallel=\frac{\gamma}{2\chi^{1D}(q_z,\omega=0;T)}\left(\frac{v}{\pi T}\right)^2, \tag{28}$$

where v is the Fermi velocity and $\gamma=2-1/2K$ is the scaling exponent of the singular part of $\chi^{1D}(q_z,\omega=0;T)$ for $T\to 0$. If T is close to T_c it follows that

$$A=A'\left(\frac{T}{T_c}-1\right), \tag{29}$$

with $A'=J\gamma$. In the Gaussian approximation,[24] the correlation length parallel to the chains is then given by

$$\xi_\parallel=\xi_{0\parallel}\left(\frac{T}{T_c}-1\right)^{-1/2}, \tag{30}$$

where the longitudinal coherence length $\xi_{0\parallel}$ is defined as

$$\xi_{0\parallel}=\sqrt{\frac{C_\parallel}{A'}}. \tag{31}$$

In the direction perpendicular to the chains, the correlation length is given by a similar expression, with

$$\xi_{0\perp}=\sqrt{\frac{C_\perp}{A'}}. \tag{32}$$

Before discussing the Ginzburg criterion, let us derive the crossover condition that has already been mentioned above. There are different criteria for the definition of a crossover condition. Here the onset of the crossover is defined as the temperature at which the perpendicular correlation length equals the distance between the chains, i.e.,

$$\xi_\perp=d_\perp. \tag{33}$$

This gives the following condition for the 1D susceptibility:

$$J'\chi^{1D}(q_z,\omega=0;T)=\frac{2}{3}. \tag{34}$$

The width of the critical region according to the Ginzburg criterion[25] is given by

$$\frac{\Delta T_c}{T_c}=\frac{1}{32(\pi\Delta C\xi_{0\perp}^2\xi_{0\parallel})^2}, \tag{35}$$

where

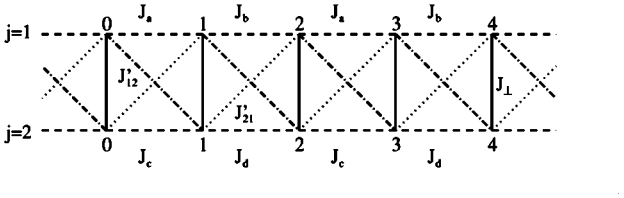

FIG. 4. The two-leg ladder with various couplings.

$$\Delta C=\frac{(A')^2}{2d_\perp^2BT_c} \tag{36}$$

is the specific heat jump per unit volume at the transition. Using the above equations, one finds

$$\frac{\Delta T_c}{T_c}\approx 0.01\frac{[J\chi^{1D}(q_z,\omega=0;T_c)]^3}{\gamma^2}. \tag{37}$$

The width of the critical region is thus of the order of 1%.

IV. TWO-LEG LADDERS AND DIMERIZED CHAINS

In this section, we derive effective Hamiltonians, describing the low-energy spectrum of various gapped spin systems that are driven into a gapless phase by an external magnetic field. First, consider a general two-leg ladder system, described by the Hamiltonian

$$H=\sum_{i,j}J_{ij}\mathbf{S}_{i,j}\cdot\mathbf{S}_{i+1,j}+J_\perp\sum_i\mathbf{S}_{i,1}\cdot\mathbf{S}_{i,2}+J'_{12}\sum_i\mathbf{S}_{i,1}\cdot\mathbf{S}_{i+1,2}$$
$$+J'_{21}\sum_i\mathbf{S}_{i,2}\cdot\mathbf{S}_{i+1,1}-h\sum_{i,j}S^z_{i,j},$$

where

$$J_{ij}=\begin{cases}J_a & \text{if } i \text{ even}, j=1\\ J_b & \text{if } i \text{ odd}, \ j=1\\ J_c & \text{if } i \text{ even}, j=2\\ J_d & \text{if } i \text{ odd}, j=2.\end{cases} \tag{38}$$

The various couplings are shown in Fig. 4. To derive the effective Hamiltonian in the gapless regime of H, a perturbation expansion in the off-rung couplings J_{ij} and J'_{ij} is performed.

Consider first the case where all couplings vanish, except for $J_\perp$. If no magnetic field is applied, the ground state of the ladder consists of independent singlets at each rung. The Hilbert-space of a single rung is spanned by the singlet $|0,0\rangle=(|\uparrow\downarrow\rangle-|\downarrow\uparrow\rangle)/\sqrt{2}$, and the triplet $|1,1\rangle=|\uparrow\uparrow\rangle$, $|1,0\rangle=(|\uparrow\downarrow\rangle+|\downarrow\uparrow\rangle)/\sqrt{2}$, $|1,-1\rangle=|\downarrow\downarrow\rangle$. The triplet excitation above the ground state is $\Delta E=1J_\perp$ for zero magnetic field. If a magnetic field is applied, the triplet states split, and for a critical field $h_{crit}=\Delta E$, the states $|0,0\rangle$ and $|1,1\rangle$ become degenerate. Upon increasing the magnetic field further, the triplet state $|1,1\rangle$ becomes the new ground state of the system. Thus at the critical field h_{crit} the magnetization changes discontinuously from zero to saturation.

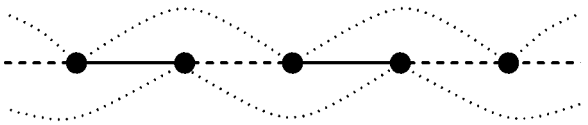

FIG. 5. The dimerized chain.

Now, consider the ladder with nonzero but small interrung couplings. The discontinuous transition for $J_\perp = 0$ is now broaded between the magnetic fields $h_{c1} < h_{crit} < h_{c2}$, and this gapless regime is described by an effective spin-1/2 Hamiltonian. To derive the corresponding effective theory for this regime, one introduces effective spin-1/2 operators $\tilde{S}_i^\alpha$ acting on the states $|\Uparrow\rangle = |1,1\rangle$ and $|\Downarrow\rangle = |0,0\rangle$ for each rung. To first order in the small couplings, one then finds an effective Hamiltonian,

$$H_{eff} = \sum_i J_i^{eff} (\tilde{S}_i^x \tilde{S}_{i+1}^x + \tilde{S}_i^y \tilde{S}_{i+1}^y + \Delta_i^{eff} \tilde{S}_i^z \tilde{S}_{i+1}^z) - \sum_i h_i^{eff} \tilde{S}_i^z, \tag{39}$$

where

$$J_i^{eff} = \frac{1}{2}(J_{i1} + J_{i2} - J'_{12} - J'_{21}), \tag{40}$$

$$\Delta_i^{eff} = \frac{1}{2} \frac{J_{i1} + J_{i2} + J'_{12} + J'_{21}}{J_{i1} + J_{i2} - J'_{12} - J'_{21}}, \tag{41}$$

$$h_i^{eff} = h - J_\perp - \frac{1}{4}(J_{i1} + J_{i2} + J'_{12} + J'_{21}). \tag{42}$$

The parameters of the effective Hamiltonian become site independent in certain cases of interest. For example, if we set $J_{ij} = J_\parallel$, we recover the known result for the strongly coupled two-leg ladder.[26] For $J_a = J_d = J_\parallel = (1-\delta)J$ and $J_b = J_c = 0$, we obtain an effective description of a single chain with dimerization δ close to one, if we set $J_\perp = (1+\delta)J$. The original model in this case is given by (see Fig. 5):

$$H_D = J \sum_i [1 + \delta(-1)^i] \mathbf{S}_i \cdot \mathbf{S}_{i+1} + J' \sum_i \mathbf{S}_i \cdot \mathbf{S}_{i+2} - h \sum_i S_i^z, \tag{43}$$

where $J' = J'_{12} = J'_{21}$ is a next-nearest-neighbor coupling constant. Note, that the isotropic chain ($\Delta_{eff} = 1$) is recovered for

$$\frac{J'}{J} = \frac{1-\delta}{6}. \tag{44}$$

In analogy to our discussion of the XXZ chain, the critical fields h_{c1} and h_{c2} can be determined for the effective Hamiltonian, i.e., $h_{c1}^{eff} = -(1+\Delta_{eff})J_{eff}$ and $h_{c2}^{eff} = (1+\Delta_{eff})J_{eff}$. Expressed in terms of the physical variables of Eq. (38), we find for the two-leg ladder:

$$h_{c1} = J_\perp - J_\parallel + \frac{J'_{12} + J'_{21}}{2}, \tag{45}$$

$$h_{c2} = J_\perp + 2J_\parallel, \tag{46}$$

and for the single dimerized chain:

$$h_{c1} = \frac{1+3\delta}{2} J + J', \tag{47}$$

$$h_{c2} = 2J. \tag{48}$$

Having derived these effective Hamiltonians, the magnetic-field driven 3D ordering temperature can be studied for the effective models, using the results of the previous sections. The behavior of the transition temperature is similar to Fig. 3(c), mainly depending on the easy-axis anisotropy Δ_{eff} of the effective model.

V. *N*-LEG LADDERS

Let us now consider the case of N-leg spin-1/2 Heisenberg ladders. If the coupling along the rungs is denoted as $J_\perp$, and the coupling along the legs as $J_\parallel$, the Hamiltonian is

$$H^N = J_\parallel \sum_{\leftrightarrow} \mathbf{S}_{i,\tau} \cdot \mathbf{S}_{j,\tau} + J_\perp \sum_{\updownarrow} \mathbf{S}_{i,\tau} \cdot \mathbf{S}_{i,\tau'}, - h \sum_{i,\tau} S_{i,\tau}^z, \tag{49}$$

where i and j enumerate the rungs, τ and τ' label the legs, and the sum marked by $\leftrightarrow$ ($\updownarrow$) runs over nearest neighbors along legs (rungs).

We first discuss the occurrence of gapless phases for these systems. Due to the alternating nature of the ground states of N-leg ladder systems at zero field, which show a spin gap for even N and are gapless for odd N, one has to consider these cases separately. In the limit of large rung coupling ($J_\perp \gg J_\parallel$), one can consider first an N-site open Heisenberg chain in a magnetic field, and then treat the coupling along the leg as a perturbation. In the case of even N, there will be $N/2$ changes in the nature of the ground state upon increasing the magnetic field. At each change, a new gapless phase opens up. This can be seen as follows: the spectrum contains multiplets of multiplicities $m = 1,3,5,\ldots,N+1$. Let $E_m(0)$ be the energy of the lowest m-plet at zero magnetic field. Then there is a gapless phase at a field

$$h_i = E_{2i+1}(0) - E_{2i-1}(0), \quad i = 1, \cdots, \frac{N}{2}. \tag{50}$$

In the case of odd N, the ground state of the system without a magnetic field is a doublet, and, therefore, the first gapless phase occurs already at $h_1 = 0$. Since the spectrum contains also multiplets with $m = 4,6,\cdots,N+1$, there are additional gapless phases at fields

$$h_i = E_{2i}(0) - E_{2i-2}(0), \quad i = 1, \ldots, \frac{N+1}{2}. \tag{51}$$

The values of the magnetic field where the gapless phases occur can, therefore, be obtained by a numerical calculation of the zero-field spectrum. In each gapless phase, there are two degenerate states, e.g., $N = 3$, $h = h_2$:

$$|\Uparrow\rangle = |\uparrow\uparrow\uparrow\rangle, \quad |\Downarrow\rangle = \frac{1}{\sqrt{6}}(|\uparrow\downarrow\downarrow\rangle - 2|\downarrow\uparrow\downarrow\rangle + |\downarrow\downarrow\uparrow\rangle).$$

TABLE II. Parameters of the effective low-energy model for the gapless regions of N-leg spin-1/2 ladders in a magnetic field h. The effective magnetic field is given by $h_{eff}=h-h_c(0)J_\perp-c_hJ_\parallel$.

N	i	$J_{eff}/J_\perp$	Δ_{eff}	$h_c(0)$	c_h
2	1	1	0.5	1	0.5
3	1	1	1	0	0
3	2	1	0.5	1.5	0.5
4	1	1.0750	0.3489	0.6589	0.375
4	2	1	0.3750	1.7071	0.625
5	1	1.0169	1	0	0
5	2	1.0961	0.3789	1.1189	0.2958
5	3	1	0.3	1.8090	0.7
6	1	1.1114	0.3163	0.4916	0.3515
6	2	1.1348	0.3011	1.3860	0.3985
6	3	1	0.25	1.8660	0.75
7	1	1.0344	1	0	0
7	2	1.1415	0.3407	0.8848	0.2166
7	3	1.1663	0.2381	1.5504	0.4891
7	4	1	0.2143	1.9010	0.7857
8	1	1.1364	0.3020	0.3926	0.3432
8	2	1.1882	0.2743	1.1506	0.2888
8	3	1.1917	0.1962	1.6577	0.5555
8	4	1	0.1875	1.9239	0.8125

For nonzero values of $J_\parallel$, these two excitations spread over the ladder in the vicinity of the critical field, thus broadening the gapless phase. To first order in $J_\parallel$, the ladder system can then be described by an effective spin-1/2 XXZ Heisenberg model in an effective magnetic field h_{eff}, after defining effective spin operators between the states $|\Uparrow\rangle$ and $|\Downarrow\rangle$ in the same matter as for the case of the two-leg ladder. Considering two such N-site chains, coupled to each other by a constant $J_\parallel$, the energy spectrum of the corresponding Hamiltonian is calculated and compared to the spectrum of the effective model. One can thus determine the values for the parameters of the effective model $(J_{eff},\Delta_{eff},h_{eff})$, where the effective magnetic field is $h_{eff}=h-h_c(0)J_\perp-c_hJ_\parallel$. The obtained values are given in Table II.

Using these effective model descriptions of the N-leg ladder in the gapless phases, we apply the RPA approach described above to a crystal of weakly coupled N-leg ladders. We now observe a cascade of $N/2$ $[(N+1)/2]$ 3D ordering transitions for quasi-1D ladder subsystems with an even (odd) number of legs, as shown in Fig. 6. In the case of weakly coupled even-leg ladders, the first transition is driven by the formation of a spin-density wave (SDW) of triplets along the ladder direction, with a ground-state wave vector that is proportional to the magnetic field $h>h_{c1}$. The following transition (for $N>2$) is driven by a SDW of quintuplets, etc. Depending on the ratio $J_\parallel/J_\perp$, these phases of different multiplet polarization may overlap, and mixed regimes can occur. The resulting 3D ordering temperature does not vanish completely in this case, but has minima at particular magnetic fields where the number of the lower multiplet excitations equals the number of the next-higher multiplet excitations. The dependence of this overlap on the ratio of the coupling constants is shown in Fig. 7, where the dark stripes show the phases of 3D order at $T=0$ for the cases

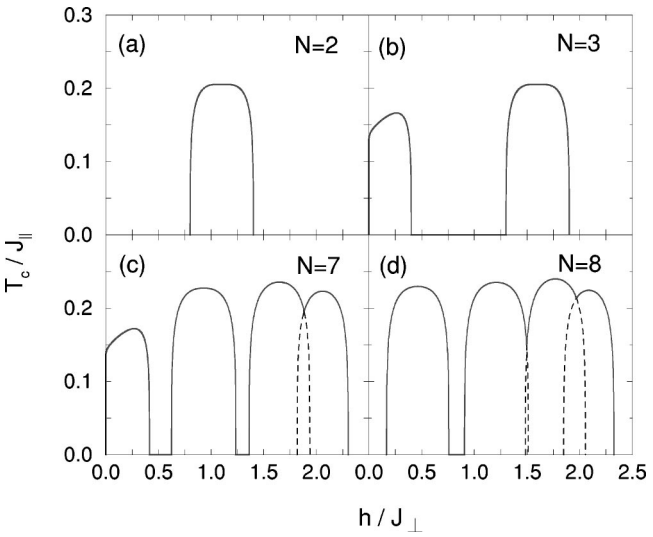

FIG. 6. 3D ordering transition temperatures of N-leg spin-1/2 Heisenberg ladders as a function of an external magnetic field. Cascades of transitions are observed for $N>2$, driven by 1D SDW's of spin-S multiplets on the ladders. For this plot, we have chosen an anisotropy ratio $J_\parallel/J_\perp=1/5$ and residual interladder coupling $J'/J_\parallel=1/16$.

$N=3, 4, 7,$ and 8. These diagrams are in good agreement with results obtained by numerical finite cluster diagonalizations.[13] Odd-leg ladders also have a sequence of ordering transitions, with the only difference that the onset of the first transition occurs already at $h=0$ [Figs. 6(b) and 6(c)].

VI. CONCLUSIONS

We have presented a theoretical approach to magnetic-field induced 3D ordering transitions in strongly anisotropic antiferromagnetically correlated spin-1/2 compounds. These systems consist of weakly coupled chains or ladders that have singlet ground states with finite excitation gaps to the

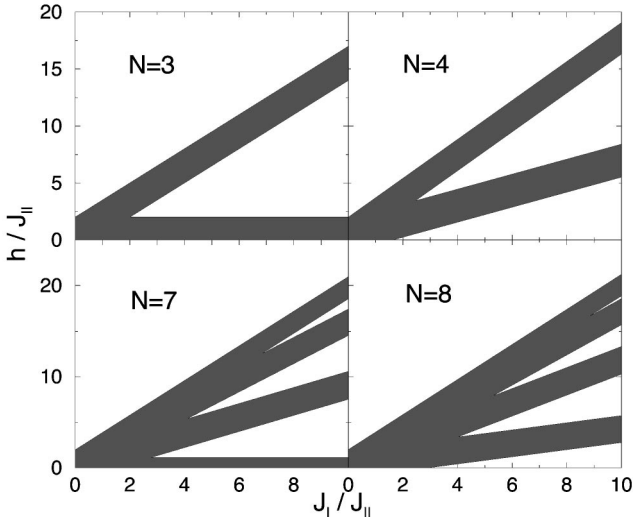

FIG. 7. Schematic phase diagrams of weakly coupled N-leg ladders in a magnetic field h at $T=0$. The shaded areas indicate 3D ordered phases, and shown is the dependence on the ratio of the ladder couplings $J_\perp/J_\parallel$.

lowest triplet states. Because the interchain couplings are weak compared to the intrachain couplings, the 1D subsystems are effectively independent. By applying an external magnetic field, the spin gap in the subsystems can be overcome, and they become partially polarized. In this incommensurate regime, even infinitesimal interchain coupling leads to 3D long-range ordering at low temperatures.

There are only a few known realizations of Bose-Einstein condensation (BEC). The two most prominent examples are ultracooled dilute ensembles of trapped atoms and the superfluid transition of helium 4. In principle, BEC can occur for any bosonic many-body system in a confining potential at low temperatures. Therefore, magnetic compounds with integer-spin excitations (e.g., spin-1 magnons) present a promising class of candidate materials. However, indications for BEC in such materials have not been found until two recent experiments on $TlCuCl_3$ and $Cu_2(C_2H_{12}N_2)_2Cl_4$. These compounds are strongly anisotropic, and have a finite spin gap Δ between their singlet ground state and the first triplet excitation. Hence, their magnetization is exponentially activated at small temperatures and zero magnetic field. An applied magnetic field can decrease the singlet-triplet excitation gaps of the 1D subsystems, and eventually drive them into a partially polarized, gapless regime if the field exceeds a critical strength. Due to residual magnetic couplings between the subsystems, a low-temperature 1D to 3D transition occurs. The resulting 3D ordering may be viewed as a BEC of spin-1 magnons, accurately predicting the temperature dependence of the critical field $[h_{\mathrm{BE}}(T)-\Delta \propto T^{2/3}]$ and the magnetization curve.[4,5]

Let us now consider multicomponent phases, as they occur in spin ladders with more than two legs. In a spin ladder, a spin-1 magnon excitation essentially corresponds to the formation of a spin triplet on a rung, a spin-2 magnon corresponds to a quintuplet, etc. At intermediate fields (larger than h_{c1}), these excitations can coexist, depending on the choice of parameters. The resulting low-temperature condensate may then contain multiple components, as it is the case at high fields in Figs. 6(c) and 6(d) (dashed regions). These phases may be viewed as multicomponent Bose-Einstein condensates, consisting of magnon excitations with different integerspins. It is, thus, of interest to conduct high magnetic field experiments on appropriate candidate materials to determine whether such phases exist in physical systems.

ACKNOWLEDGMENTS

S.W. acknowledges support from DAAD under Grant Number HSP III,D/98/11174, S.H. was supported by the Zumberge Foundation.

[1] H. J. Schulz, Phys. Rev. Lett. **77**, 2790 (1996).
[2] S. Haas and M. Sigrist, in *Physical Phenomena at High Magnetic Fields III*, edited by J.R. Schrieffer, L. Gorkov, and Z. Fisk (World Scientific, Singapore, 1999).
[3] S. Wessel and S. Haas, cond-mat/9905331, Eur. Phys. J. B (to be published).
[4] T. Giamarchi and A. M. Tsvelik, Phys. Rev. B **59**, 11 398 (1999).
[5] T. Nikuni, M. Oshikawa, A. Oosawa, and H. Tanaka, cond-mat/9908118 (unpublished).
[6] G. Chaboussant, Y. Fagot-Revurat, M.-H. Julien, M. E. Hanson, C. Berthier, M. Horavitć, L. P. Lévy, and O. Piovesana, Phys. Rev. Lett. **80**, 2713 (1998); Eur. Phys. J. B **6**, 167 (1998).
[7] C. Broholm (private communication).
[8] N. Cavadini, W. Henggeler, A. Furrer, H.-U. Güdel, K. Krämer, and H. Mutka, Eur. Phys. J. B **7**, 519 (1999).
[9] M. Hase, I. Terasaki, and K. Uchiokura, Phys. Rev. Lett. **70**, 3651 (1993).
[10] D. Augier, D. Poiblac, S. Haas, A. Delia, and E. Dagotto, Phys. Rev. B **56**, R5732 (1997).
[11] M. Azuma, Z. Hiroi, M. Takano, K. Ishida, and Y. Kitaoka, Phys. Rev. Lett. **73**, 3463 (1994); Z. Hiroi, M. Azuma, M. Takano, and Y. Baudo, J. Solid State Chem. **95**, 230 (1991).
[12] F. D. M. Haldane, Phys. Rev. Lett. **45**, 1358 (1980).
[13] D. C. Cabra, A. Honecker, and P. Pujol, Phys. Rev. Lett. **79**, 5126 (1997); Phys. Rev. B **58**, 6241 (1998).
[14] P. Jordan and E. Wigner, Z. Phys. **47**, 631 (1928).
[15] V. E. Korepin, N. M. Bogoliubov, and A. G. Izergin, *Quantum Inverse Scattering Method and Correlation Functions* (Cambridge University Press, Cambridge, England, 1993).
[16] S. Qin, M. Fabrizio, L. Yu, M. Oshikawa, and I. Affleck, Phys. Rev. B **56**, 9766 (1997).
[17] There are slight differences between our functions and those given in Ref. 13.
[18] H. J. Schulz, Phys. Rev. B **34**, 6372 (1986).
[19] R. Chitra and T. Giamarchi, Phys. Rev. B **55**, 5816 (1997).
[20] S. Lukyanov and A. B. Zamolokchiov, Nucl. Phys. B **493**, 571 (1997).
[21] J. Jensen and Allan R. Mackintosh, *Rare Earth Magnetism* (Oxford University Press, New York, 1991).
[22] A more careful treatment should take into consideration that the dispersion at the bottom of the spinless fermion band is quadratic. See, e.g., T. Giamarchi and A. M. Tsvelik, Phys. Rev. B **59**, 11 398 (1999). In this case, a modified exponent, $\alpha=2/3$, is obtained.
[23] N. Menyhard, J. Phys. C **11**, 2207 (1978).
[24] R. H. McKenzie, Phys. Rev. B **52**, 16 428 (1995).
[25] V. L. Ginzburg, Fiz. Tverd. Tela (Leningrad) **2**, 2031 (1961) [Sov. Phys. Solid State **2**, 1824 (1960)].
[26] F. Mila, Eur. Phys. J. B **6**, 210 (1998).